Fusion Engineering and Design 146 (2019) 2639–2643

Contents lists available at ScienceDirect

Fusion Engineering and Design

journal homepage: www.elsevier.com/locate/fusengdes

The JET upgraded toroidal Alfvén Eigenmode Diagnostic System

S. Dowson[a,g,*], S. Dorling[a,g], H.K. Sheikh[a,g], T. Blackman[a,g], G. Jones[a,g], A. Goodyear[a,g], P. Puglia[b,g], P. Blanchard[b,g], A. Fasoli[b,g], D. Testa[b,g], N. Fil[c,g], V. Aslanyan[c,g], M. Porkolab[c,g], P. Woskov[c,g], W. Pires De Sa[d,g], R. Galvao[d,g], L. Ruchko[d,g], J. Figueiredo[e,f,g], C. Perez Von Thun[e,g], JET Contributors[1]

[a] CCFE, Culham Science Centre, Abingdon, OX14 3DB, United Kingdom
[b] EPFL Swiss Plasma Center, Lausanne, Switzerland
[c] MIT PSFC, 175 Albany Street, Cambridge, MA 02139, United States
[d] Instituto de Física, Universidade de São Paulo, São Paulo CEP 05508-090, Brazil
[e] EUROfusion PMU, Culham Science Centre, Abingdon, Oxon, OX 14 3DB, United Kingdom
[f] Instituto de Plasmas e Fusão Nuclear, Instituto Superior Técnico, Universidade de Lisboa, Portugal
[g] EUROfusion Consortium, JET, Culham Science Centre, Abingdon, OX14 3DB, United Kingdom

ARTICLE INFO

Keywords:
JET
TAE
FPGA
FPAA
AEAD
Alfvén

ABSTRACT

The Alfvén Eigenmode Active Diagnostic system (AEAD) has undergone a major upgrade and redesign to provide a state-of-the-art excitation and real-time detection system for JET.

The new system consists of individual 4 kW amplifiers allowing for increased current, separate excitation and real time control of relative phasing between antenna currents. The amplifiers have a frequency range of 10–1000 kHz, divided into various frequency bands by external matching filters. Due to the varying transmission line impedance throughout the frequency range, the amplifiers were designed with a very high resilience to reflected power.

The existing amplifier control electronics have been replaced with a digital control system incorporating a National Instruments platform and Field Programmable Gate Array (FPGA) modules for frequency, gain and phase control with a frequency and phase resolution of less than 1 kHz and 1 degree respectively. Complementing the digital control system is the Protection and Control System, which utilizes Field Programmable Analog Arrays (FPAAs) and an array of electronic devices to monitor and control the AEAD.

New capabilities such as independent antenna current/phase control, allow for improved excitation control, better definition of antenna spectrum combined with enhanced system reliability. This paper will review the new AEAD system, its unique capabilities and improvements over the previous diagnostic system.

1. Introduction

The JET Alfvén Eigenmode Active Diagnostic (AEAD) probes the background Alfvén Eigenmodes (AEs) spectra of the plasma [1]. It does so by resonantly exciting AEs [2,3] via two antenna modules, with each module housing four excitation coils. The Antenna modules are separated by 180° toroidally.

Previously the excitation coils were driven by a single, high power broadband amplifier, with a maximum power output of 5 kW within a frequency band of 10–500 kHz. The previous system successfully measured damping rates for toroidal mode numbers, $n \leq 7$ though unfortunately struggled to measure damping rates for modes $n \geq 8$ [4–6]. Two factors strongly influenced the difficulty in exciting and characterising high-n modes: (1) These modes have a quasi-degenerate spectrum and radial eigenfunctions peaked towards the centre of the plasma column, i.e. away from the antennae. (2) The capability to optimize the antenna phase currents (only 0 and π were possible) to excite certain n modes was severely restricted.

To overcome these restrictions and allow for the probing of AEs in plasma configurations that were not possible to probe in the past, a new upgraded system was proposed in preparation for the deuterium–-tritium (DT) campaign. In the new system described here, each

* Corresponding author at: CCFE, Culham Science Centre, Abingdon, OX14 3DB, UK.
E-mail address: stuart.dowson@ukaea.uk (S. Dowson).

[1] See the author list of "Overview of the JET preparation for Deuterium-Tritium Operation" by E. Joffrin et al. to be published in Nuclear Fusion Special issue: overview and summary reports from the 27th Fusion Energy Conference (Ahmedabad, India, 22-27 October 2018).

https://doi.org/10.1016/j.fusengdes.2019.04.064
Received 10 October 2018; Received in revised form 15 April 2019; Accepted 15 April 2019
Available online 25 April 2019
0920-3796/

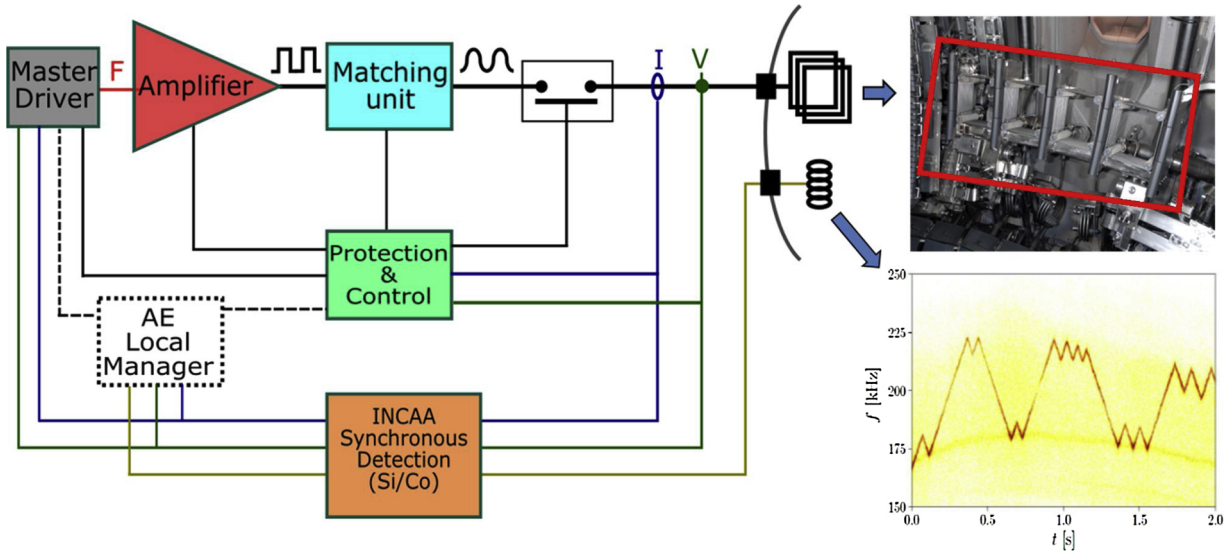

Fig. 1. A schematic overview of the AEAD system. Antenna (top right) and spectrogram showing tracking of AEs (bottom right). The INCAA synchronous detection system applies a frequency mixer with the synchronous in-phase (I) and quadrature (Q) components of the antenna signal to the incoming differential signals which are then filtered by a low-pass filter with a < 100 Hz bandwidth, generating their corresponding cosine (I) and sine (Q) DC components that are used by both the MD and the AE local manager for phase and current measurement as well as phase and current control. The MD drives the RF amplifiers with a small, frequency swept square-wave signal, which in turn is amplified by the amplifiers. The matching units (low pass filters) then smooth out the amplifier output, resulting in a sinusoidal wave which is then transmitted via co-axial cables (approx. 85 m in length) to the antennas. The protection and control block is at the centre of the system, interconnecting with all system elements and responsible for trip management and protection of the AEAD system as well as timing and signal processing.

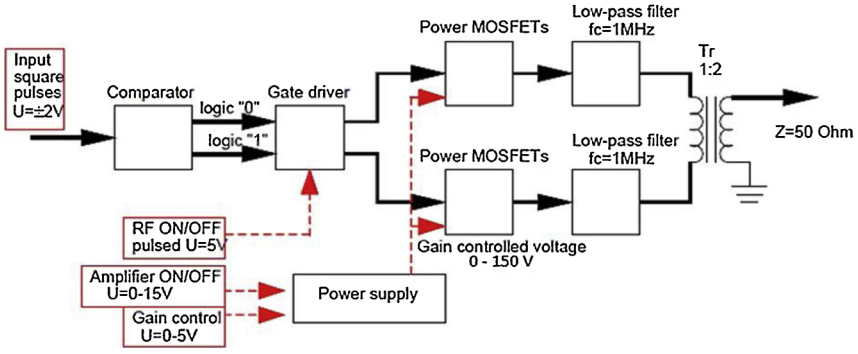

Fig. 2. Block diagram of RF circuit.

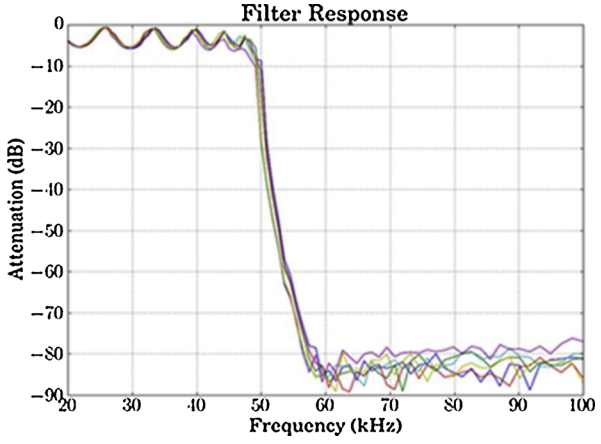

Fig. 3. Frequency response of 50 kHz filter.

excitation coil is now driven by a single 4 kW amplifier; allowing for increased current, separate excitation and real time control of relative phasing between antenna currents with an extended frequency range of 10–1000 kHz.

In this paper, Section 2 describes the new AEAD system in-depth, with a strong focus on the new elements of the system. Section 3 reviews the operation of the AEAD system and its performance thus far.

2. AEAD upgrade

The system upgrade essentially consists of individual RF amplifiers driving the in-vessel excitation coils. The RF amplifiers are driven and controlled by what is known as the Master Driver (MD) which is essentially a National Instruments (NI) PXI express chassis incorporating LabView Real Time (RT) and Field Programmable Gate Array (FPGA) software.

The total system power has increased from 5 kW to 24 kW (4 kW/Amplifier – at present six amplifiers installed driving six excitation coils), with the bandwidth being extended to 1000 kHz to allow for MHD spectroscopy using global Alfvén waves below the continuum [7].

A schematic overview of the new system and spectrogram showing tracking of AEs [8] is shown in Fig. 1.

2.1. RF amplifiers and filters

The RF amplifier is based upon a metal–oxide–semiconductor field-

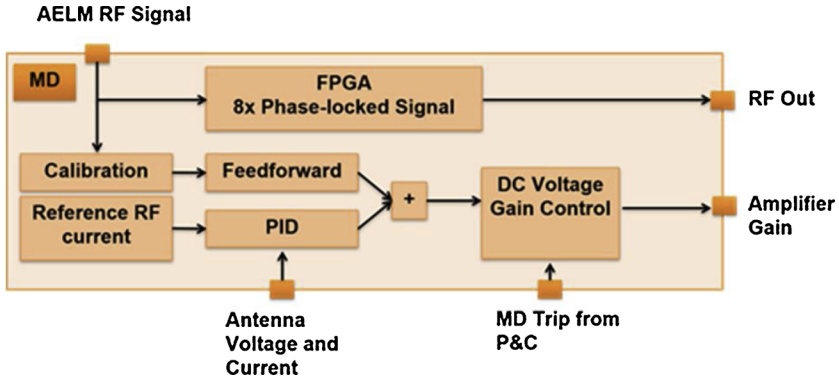

Fig. 4. Master Driver block diagram.

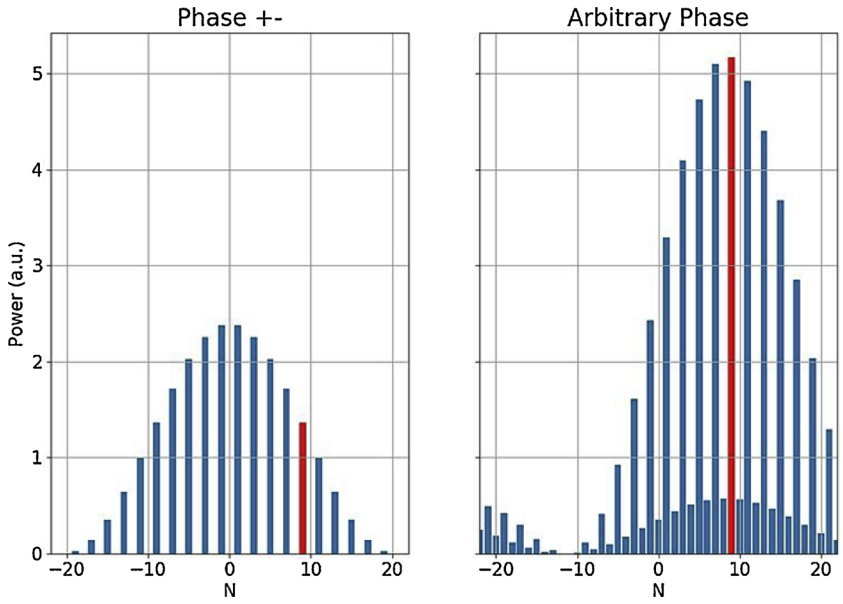

Fig. 5. Calculation illustrating arbitrary phase optimization for specific mode excitation with six antennas.

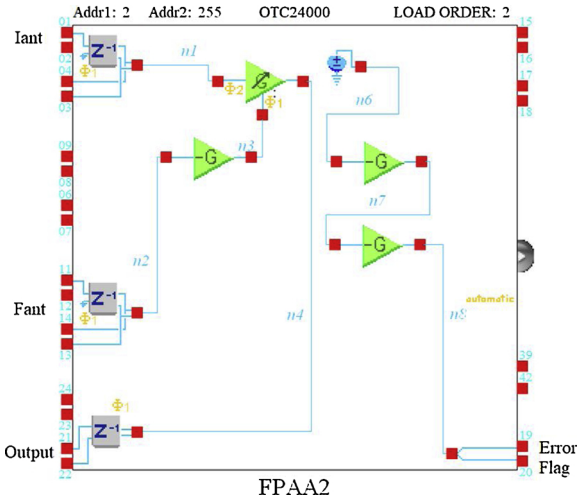

Fig. 6. Software for measurement of antenna current.

effect transistor (MOSFET) switching/push-pull scheme (Fig. 2.) classified as a class-D amplifier, with a bandwidth of 10–1000 kHz. Due to the varying transmission line impedance throughout the frequency range, the amplifiers were designed with a very high resilience to reflected power with a Voltage Standing Wave Ratio VSWR > > 10:1. This allows for fast frequency sweeping without tripping the amplifiers, resulting in a reliable, robust system free of nuisance tripping.

The frequency range of 10–1000 kHz is divided into various frequency bands by external matching filters. The matching filters are 18th order, Chebyshev low pass filters that convert/smooth out the amplifier square-wave output to a sinusoidal wave and attenuate (by at least 70 dB) the third harmonics. The filters have been designed in this way as the synchronous detection system is sensitive to third harmonics and will not operate correctly in their presence. The frequency response of the 50 kHz filter is shown in Fig. 3. with an attenuation of $\approx 80\,dB$. Three filters are currently in use: 50, 150 and 250 kHz (f_c) with the bandwidth of each filter being $f_c/2$.

2.2. Master driver

The Master Driver (MD) hardware for the JET AEAD system upgrade is based on a National Instruments (NI) PXI express chassis, Model PXIe-1075 with 18 slots. It includes an Intel i7 quad-processor embedded computer, five NI modules, and three custom signal conditioning boards fabricated at MIT. LabView Real Time (RT) and Field Programmable Gate Array (FPGA) software is implemented in the system for performing the various amplifier input and control functions, which include phase-controlled frequency swept drives to the amplifiers and amplifier gain control (Fig. 4.). The amplifier drive signals are generated in the FPGA module by a direct digital synthesis (DDS) algorithm controlled by an external swept voltage that is input to one of

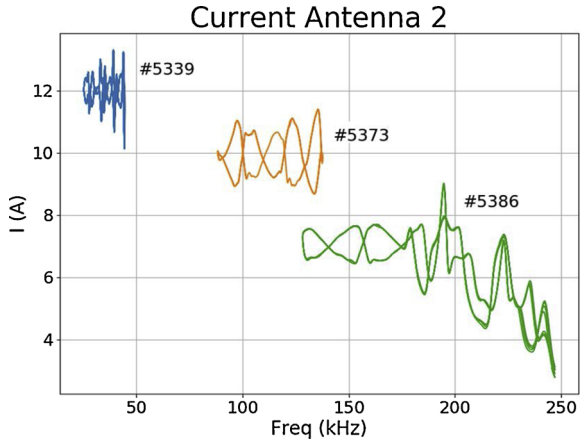

Fig. 7. Current measured in frequency bands; 50, 150 and 250 kHz for offline shots (#).

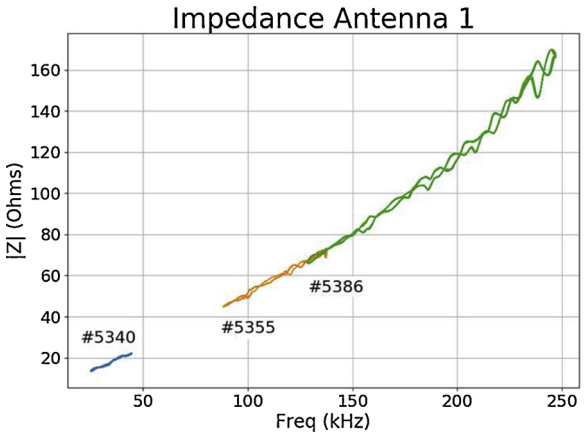

Fig. 9. Impedance calculated from Antenna voltage and currents in frequency bands 50, 150 and 250 kHz for offline shots (#).

the DAQ channels. The FPGA board generates $1GS.s^{-1}$ of data points, which gives a frequency resolution of 1 Hz and a phase resolution of 0.3 degrees at 100 kHz.

The previous system used only one amplifier to drive all antennas allowing for only 0 and π phase control (+/- Phase). This configuration led to n-spectra symmetrical around $n = 0$ (Fig.5. LHS). Thanks to the upgrade, each RF amplifier independently excites each antenna allowing for arbitrary phase control between antenna currents and hence excitation of a particular toroidal mode number up to $|n| = 15$ (Fig. 5. RHS).

2.3. Protection and control

Complementing the digital control system, the Protection and Control System is responsible for trip management and protection of the AEAD system as well as timing and signal processing. Field Programmable Analog Arrays (FPAA) have been utilised for the signal processing and precise measurement of antenna voltage and antenna current.

The FPAA incorporates a 2×2 matrix of Configurable Analogue Blocks (CAB) surrounded by programmable interfaces and analogue input/output cells with active elements. Analogue signal processing is accomplished using an architecture based on switched capacitor circuit design. Every CAB contains two op-amps, a comparator, banks of programmable capacitors, and a collection of configurable routing and clock resources. The FPAA can be thought of as the analogue equivalent to the FPGA.

Circuit design is via Dynamx Design Lab software [9], a graphical design environment in which analogue signal processing blocks are connected together. Building blocks include; amplifiers, multipliers, summing blocks, integrators and other specialised bocks. Specific behaviours for each of the blocks are set by the user.

For each antenna three FPAAs are daisy-chained together for the measurement of antenna voltage, current and earth leakage current. The software for each of these measurements is identical with only the coefficients in the Look Up Table (LUT) changing (Fig. 6.)

The FPAA monitors the measured signal in and frequency reference. Due to the mismatch on the measurement lines and large frequency sweep/bandwidth of system, the output from the voltage and current measurement coils varies with frequency. The Variable Gain Amplifier (VGA) refers to the LUT and selects the correct gain coefficient according to the frequency. Two clocks are required for the multiplier CAB, a relatively slow one for the gain stage (measured signal input – 1 MHz) and a second faster one, 16 times faster for the ADC (frequency reference input – 16 MHz). The 16:1 clock ratio required arises from the required time for ADC processing. The software also monitors the internal reference voltage, which in the event of FPAA failure, will go to zero, thus producing an error flag. Fig. 8. shows the signal processing path of the measurement signals.

3. System performance and operation

The AEAD diagnostic has been successfully commissioned with the latest enhancements and operated up to the limits imposed by the transmission line feedthroughs on the JET vessel (1.1 kV and 15 A). Due to the inductance of the antennas, the maximum current that can be driven in each coil is dictated by the frequency band of operation and the feedthrough voltage limit (Fig. 7.). The impedance of the antenna can be calculated from the voltages and currents measured (Fig. 9).

Real time phase control with frequency sweeps at 200 kHz/s on various antennas has been demonstrated successfully (Fig. 10). Small spikes can be seen in the phase control however the MD control loops are still being optimised for peak performance.

4. Conclusion

In summary, the AEAD has been successfully upgraded and shown to be a robust and reliable system capable of detecting and tracking modes. Increased power (≈ 5x that of previous system) and real time phase control will allow for mode number identification up to $|n| \leq 15$.

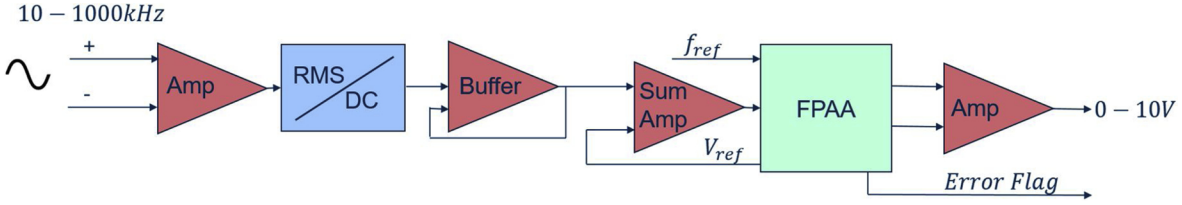

Fig. 8. Signal path of measurement signal shown. Raw signal is converted to RMS then peak value is recovered before being buffered and then summed with FPAA reference voltage. This off-set/addition is necessary to ensure the signal is within the acceptable range for the FPAA. The final output is a 0–10 V signal out representing measurement signal in.

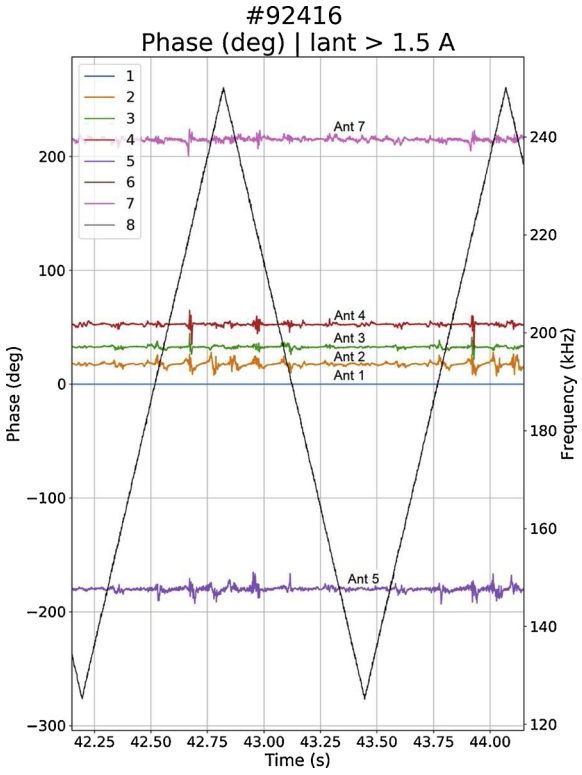

Fig. 10. Real time phase control during frequency sweep at 200 kHz/s.

Possible further work would be to implement phase two of the project; a new FPGA based digital synchronous detection system with a frequency range of 1000 kHz and the ability to excite and track in real time simultaneously different mode numbers.

Acknowledgments

This work has been carried out within the framework of the EUROfusion Consortium and has received funding from the Euratom research and training programme 2014–2018 under grant agreement No. 633053. The views and opinions expressed herein do not necessarily reflect those of the European Commission'. The Brazilian group works under the scientific agreement for cooperation between the European Atomic Energy Community and the Government of the Federative Republic of Brazil in the field of fusion energy research and has been supported by the Brazilian agencies FAPESP, Project 2011/50773-0, and CNPq, Project 480733/2013-9. The work of the US collaborators at MIT was supported by the US DOE Grant DE-FG02-99ER54563. This work was also supported in part by the Swiss National Science Foundation.

References

[1] A. Fasoli, et al., Plasma Phys. Control. Fusion 44 (2002) B159.
[2] D. Testa, et al., Proc. 23rd SOFT 143354 (2005).
[3] D. Testa, et al., Nucl. Eng. 50 (2010) 084010.
[4] T. Panis, A. Fasoli, D. Testa, et al., Nucl. Eng. 52 (2012) 023013.
[5] T. Panis, A. Fasoli, D. Testa, et al., Nucl. Eng. 52 (2012) 023014.
[6] D. Testa, et al., Europhys. Lett. 92 (2010) 50001.
[7] P. Puglia, et al., Phys. Plasmas 21 (2016) 122509.
[8] D. Testa, et al., EPL 92 (2010) 50001.
[9] Okika Technologies, (2018) (26/09/2018), https://okikatechnologies.com/.